THE NONADIABATIC ANALYSIS OF NONRADIAL MODES OF STELLAR OSCILLATION IN THE PRESENCE OF SLOW ROTATION

BRADLEY W. CARROLL[1] AND CARL J. HANSEN
Joint Institute for Laboratory Astrophysics, University of Colorado and National Bureau of Standards; and
the Departments of Physics and Astro-geophysics, University of Colorado

ABSTRACT

The linearized equations governing nonadiabatic, nonradial pulsations of a slowly but uniformly rotating star have been derived. A large number of numerical examples are presented for near main sequence evolution of a 12 $M_\odot$ star. All modes with $l = 2$ and 3 and with periods between two and 15 hours were examined for this sequence. Other masses and values of l were studied, but to a lesser extent. For all modes and sequences studied it was found that slow, uniform rotation increases the pulsation frequency (as observed from an inertial frame) of prograde modes ($m < 0$), and conversely for retrograde modes. The effect of rotation on stability is not as clear-cut. On the main sequence it enhances the stability of retrograde modes and makes prograde modes less stable. As evolution progresses, this distinction becomes less strong. Possible implications for β Cephei and line profile variables are discussed.

Subject headings: line profiles — stars: β Cephei — stars: pulsation — stars: rotation

I. INTRODUCTION

In an earlier paper, Hansen, Cox, and Carroll (1978, hereafter HCC) used a quasi-adiabatic analysis in an investigation of the effect of slow, uniform rotation on the pulsational stability of stellar models. They found, for iron white dwarfs and upper zero-age main-sequence stars, and for those pulsation modes considered, that rotation enhances the stability of the retrograde ($m > 0$) modes and diminishes the stability of the prograde ($m < 0$) modes. Here m is the azimuthal spherical harmonic index. The present work extends that of HCC to a fully nonadiabatic treatment.

For slow rotation, terms involving powers of Ω (the angular rotation frequency) higher than the first are neglected. Rotation then acts only through the Coriolis force; the centrifugal force is ignored completely. This means that the unperturbed (nonpulsating) model is that of a nonrotating star. In this paper, it is taken to be a spherically symmetric, static model of a star in hydrostatic and thermal equilibrium, with no meridional currents or magnetic fields present. The assumption of uniform (solid body) rotation is almost certainly unrealistic. Still, it is hoped that the results obtained using this assumption will be at least qualitatively correct. For an adiabatic treatment of this problem using a differential rotation law, see Hansen, Cox, and van Horn (1977).

In this paper we shall work exclusively in the intertial frame. For a uniformly rotating star (as considered here) the corotating frame is computationally simplier but our aim is to present the analysis in such a fashion that the

extension to nonuniformly rotating stars, though not simple, may be made apparent.

In § II the basic equations are developed; they are then "second linearized" in § III in order to isolate effects proportional to the rotation frequency Ω. Integral expressions for the stability coefficient are described in § IV. Section V discusses the normalization procedure adopted for the second linearized equations, and § VI contains the results of the numerical solution of these equations. An Appendix is included which gives the full set of second linearized equations and their boundary conditions along with expressions for the surface velocity field. This latter analysis may prove useful for the interpretation of observational data.

II. BASIC EQUATIONS

The equations that determine the nonradial, nonadiabatic motions of a star are

$$\frac{\partial \rho}{\partial t} + \nabla \cdot \rho \boldsymbol{v} = 0 , \tag{1}$$

$$\rho \frac{d^2 \boldsymbol{r}}{dt^2} = -\nabla P - \rho \nabla \psi , \tag{2}$$

$$T \frac{ds}{dt} = \epsilon - \frac{1}{\rho} \nabla \cdot \boldsymbol{F} , \tag{3}$$

$$\nabla^2 \psi = 4\pi G \rho , \tag{4}$$

where all symbols have their usual meaning. The energy flux $\boldsymbol{F}$ is the sum of the radiative and convective contributions

$$\boldsymbol{F} = \boldsymbol{F}_{\mathrm{rad}} + \boldsymbol{F}_c .$$

[1] Presently at the University of Rochester.

In the Eddington approximation

$$F_{\text{rad}} = -\frac{4\pi}{3\kappa\rho} \nabla J ,\qquad (5)$$

which is valid in both the optically thick and thin limits (Unno and Spiegel 1966). Unno (1965) expresses J as

$$J = \frac{ac}{4\pi} T^4 + \frac{1}{4\pi\kappa} T \frac{ds}{dt} .\qquad (6)$$

The time derivative d/dt in the above equations is the Stokes or comoving derivative,

$$\frac{d}{dt} = \frac{\partial}{\partial t} + V \cdot \nabla = \frac{\partial}{\partial t} + M ,\qquad (7)$$

which defines the operator M. For a uniformly rotating star, $v = \Omega r \sin \theta \hat{\phi}$ (spherical coordinates), so that

$$\frac{d}{dt} = \frac{\partial}{\partial t} + \Omega \frac{\partial}{\partial \phi} .$$

As usual, the Lagrangian variation δf and Eulerian variation f' of scalar quantities f are written as

$$\delta f(\mathbf{r}, t) = \delta f(r) Y_l^m(\theta, \phi) e^{i\sigma t} ,$$

$$f'(\mathbf{r}, t) = f'(r) Y_l^m(\theta, \phi) e^{i\sigma t} ,$$

where σ is the complex pulsation frequency and the Y_l^m are the spherical harmonic functions. Furthermore, the Lagrangian displacement $\delta \mathbf{r}$ of a mass element from its equilibrium position is written as

$$\delta \mathbf{r}(\mathbf{r}, t) = \boldsymbol{\xi}(\mathbf{r}) e^{i\sigma t} .$$

The components of $\delta \mathbf{r}$, to first order in Ω, come from the linearized version of the momentum equation (2):

$$-(\sigma^3 + 6m\sigma^2\Omega)\xi_r = (\sigma + 4m\Omega)\gamma(r)Y_l^m + 2m\Omega\beta(r)Y_l^m ,\qquad (8)$$

$$-(\sigma^3 + 6m\sigma^2\Omega)\xi_\theta = (\sigma + 4m\Omega)\beta(r)\frac{\partial}{\partial\theta} Y_l^m$$
$$+ 2m\Omega \frac{\cos\theta}{\sin\theta} \beta(r)Y_l^m ,\qquad (9)$$

$$-(\sigma^3 + 6m\sigma^2\Omega)\xi_\phi = (\sigma + 4m\Omega)\frac{im}{\sin\theta}\beta(r)Y_l^m$$
$$+ 2i\Omega\left[\sin\theta\gamma(r)Y_l^m + \cos\theta\beta(r)\frac{\partial}{\partial\theta} Y_l^m\right] .\qquad (10)$$

In the above,

$$\gamma(r) = -\frac{d}{dr}\chi(r) + \frac{\Gamma_3 - 1}{\Gamma_1} \frac{\rho g}{P} T\delta s(r)$$
$$- A[\chi(r) - \psi'(r) - g\xi_r(r)] ,$$

and

$$\beta(r) = -\frac{1}{r}\chi(r) ,$$

where

$$\chi(r) = \frac{P'(r)}{\rho} + \psi'(r)$$

and A is the convective stability factor

$$A = \frac{1}{\rho}\frac{d\rho}{dr} - \frac{1}{\Gamma_1 P}\frac{dP}{dr} .$$

For zero rotation, these equations reduce to the usual form

$$\xi_r = a_0(r)Y_l^m ,\qquad (11)$$

$$\xi_\theta = b_0(r)\frac{\partial}{\partial\theta} Y_l^m ,\qquad (12)$$

$$\xi_\phi = \frac{im}{\sin\theta} b_0(r)Y_l^m\qquad (13)$$

(see, for example, § 82 of Ledoux and Walraven 1958). This defines a class of modes called the spheroidal modes. Another possible class, the toroidal modes, is defined by the solution set

$$\xi_r = 0 ,$$

$$\xi_\theta = +\frac{im}{\sin\theta}\frac{T(r)}{r} Y_l^m , \quad \xi_\phi = -\frac{T(r)}{r}\frac{\partial}{\partial\theta} Y_l^m .$$

This separation of mode types is thoroughly discussed by Aizenman and Smeyers (1977), who also show that toroidal modes with $\sigma \neq 0$ exist only in a rotating star. The spheroidal and toroidal modes together form a complete set. The complicated angular dependencies of ξ_θ and ξ_ϕ in equations (9) and (10) show that the eigenfunctions of a rotating, pulsating star must be an admixture of spheroidal and toroidal modes. As a result, the velocity of a mass element in such a star can not be simply expressed as the sum of a zero-rotation velocity plus the rotational velocity $\Omega r \sin \theta \hat{\phi}$ (see Appendix).

Following Saio and Cox (1980), the linearized versions of equations (1)–(6) may be manipulated to produce six complex first-order differential equations and seven associated boundary conditions (three at the stellar center, three at the surface, plus an arbitrary normalization). These are written in terms of the dimensionless variables

$$y_1 = \frac{1}{r}\xi_r , \quad y_2 = \frac{1}{gr}\left(\frac{P'}{\rho} + \psi'\right) , \quad y_3 = \frac{1}{gr}\psi' ,$$

$$y_4 = \frac{1}{g}\frac{d\psi'}{dr} , \quad y_5 = \frac{1}{C_p}\delta s , \quad y_6 = \frac{1}{L_{\text{rad}}}\delta L_{\text{rad}} ,$$

and the dimensionless frequencies

$$\omega^2 = \frac{R^3}{GM}\sigma^2 , \quad \Sigma^2 = \frac{R^3}{GM}\Omega^2 .\qquad (14)$$

For the purpose of this paper, it is sufficient to give only the equations for y_1 and y_2:

$$r\frac{dy_1}{dr} = \left[\frac{V}{\Gamma_1} - 3 + \frac{2m\Sigma}{\omega}\right]y_1$$
$$+ \left[\frac{l(l+1)}{C_1\omega^2}\left(1 - \frac{2m\Sigma}{\omega}\right) - \frac{V}{\Gamma_1} + \frac{1}{C_1\omega^2}\frac{2m\Sigma}{\omega}\right]y_2$$
$$+ \frac{V}{\Gamma_1}y_3 + \frac{\chi_T}{\chi_\rho}y_5 , \tag{15}$$

$$r\frac{dy_2}{dr} = \left[C_1\omega^2\left(1 + \frac{2m\Sigma}{\omega}\right) + rA\right]y_1$$
$$+ \left[1 - U - rA - \frac{2m\Sigma}{\omega}\right]y_2 + rAy_3 + \frac{\chi_T}{\chi_\rho}y_5 . \tag{16}$$

The notation used here is identical to that of Saio and Cox (1980).

III. SECOND LINEARIZATION

In order that effects proportional to Ω may be isolated, the eigenfunctions y_i ($i = 1, \ldots, 6$) and dimensionless eigenfrequency ω are written as the sum of a zero-rotation part (zero subscript) plus a rotational correction (barred), assumed small for the case of slow rotation

$$y_i = y_{i0} + \bar{y}_i , \quad \omega = \omega_0 + \bar{\omega} . \tag{17}$$

(This follows the treatment of HCC.) Furthermore, $\bar{\omega}$ is expressed as

$$\bar{\omega} = -m\Sigma(1 - C) . \tag{18}$$

It is the complex number C which will be solved for as an eigenvalue. If the pulsation frequency is written as the sum of real (r) and an imaginary (i) parts,

$$\sigma = \sigma_r + i\kappa ,$$

where κ is the stability coefficient, then

$$\bar{\sigma}_r = -m\Omega(1 - C_r) , \tag{19}$$

$$\bar{\kappa} = m\Omega C_i . \tag{20}$$

If $\bar{\kappa}$ is negative, then rotation is a destabilizing influence.

Relations (17) and (18) are introduced into the six differential equations and their associated boundary conditions, and terms proportional to powers of Ω higher than the first are discarded. This yields another, and rather complicated, set of six differential equations and boundary conditions, which are given in the Appendix. If $\Sigma = 0$, these equations and boundary conditions are identical to the zero-rotation equations of Saio and Cox (1980). Once ω_0 and the y_{i0} are known (by solving the zero-rotation equations), they are used to determine the rotational corrections $\bar{\omega}$ (or equivalently, C) and the $\bar{y}_i$. Note that the eigenfunctions for the second linearized equations scale as $2m\Sigma/\omega_0$. That is, the quantities actually solved for are $\bar{y}_i/(2m\Sigma/\omega_0)$.

Unlike the zero-rotation equations of Saio and Cox, these second linearized equations are not homogeneous.

This means that the normalization of the $\bar{y}_i$ is not arbitrary. A discussion of the normalization procedure will be deferred to § V.

IV. INTEGRAL EXPRESSIONS

An integral expression for the stability coefficient provides an important check on the consistency of the numerical solution of the differential equations. The eigenvalue κ and the value of κ derived from an integral procedure should agree within the limits of computational accuracy. Our starting point is equation (37) of Aizenman and Cox (1975), written as

$$-\sigma^3 J + \sigma^2 R_1 + \sigma\ddot{R} - R_2 = iN , \tag{21}$$

where

$$J = \int \rho\xi^* \cdot \xi d^3r , \quad R_1 = 3i\int \rho\xi^* \cdot M(\xi)d^3r ,$$

$$\ddot{R} = \int \xi^* \cdot [P(\xi) + V(\xi)]d^3r ,$$

$$R_2 = i\int \rho\xi^* \cdot M\left\{\frac{1}{\rho}[P(\xi) + V(\xi)]\right\}d^3r ,$$

$$N = \int \rho\xi^* \cdot \left[\frac{d}{dt}\left(\frac{1}{\rho}\nabla\Psi\right)\right]_{sp}d^3r .$$

In the above, M is as defined by equation (7), P and V are as given in Aizenman and Cox, and Ψ is the nonadiabatic contribution

$$\Psi = \delta P - \frac{\Gamma_1 P}{\rho}\delta\rho .$$

(The "sp" subscript means "space part.") The integrals J, R_1, and $\ddot{R}$ are all real; this last by the Hermiticity of the operators P and V (Lynden-Bell and Ostriker 1967). Aizenman and Cox show that, for slow, uniform rotation, the nonadiabatic contribution N is given by

$$N = C - H ,$$

where C is the usual work integral

$$C = \int \rho(\Gamma_3 - 1)\left(\frac{\delta\rho}{\rho}\right)^* T\left[\frac{d}{dt}\delta s\right]_{sp}d^3r ,$$

and

$$H = \int [(\xi^* \cdot \nabla)v_0] \cdot (\nabla\Psi)d^3r .$$

For the case of zero rotation, equation (21) reduces to

$$-\sigma_0^3 J_0 + \sigma_0\ddot{R}_0 = iC_0 . \tag{22}$$

Writing σ_0 and C_0 as the sums of real and imaginary parts,

$$\sigma_0 = \sigma_{0r} + i\kappa_0 , \quad C_0 = C_{0r} + iC_{0i} ,$$

leads to an expression for κ_0:

$$\kappa_0 = \frac{-C_{0r}}{\frac{8}{3}\sigma_{0r}^2 J_0 + \frac{1}{3}\sigma_{0r}^{-1}C_{0i} - \frac{2}{3}\ddot{R}_0} . \tag{23}$$

If nonadiabatic effects are small, this reduces to the usual result

$$\kappa_0 = \frac{-C_{0r}}{2\sigma_{0r}^2 J_0}. \tag{24}$$

However, equation (23) is an identity, while equation (24) is only an approximation (albeit a very good one in most cases).

An expression for the rotational correction to the complex pulsation frequency may be found by writing each quantity (except R_1 and R_2 which are already proportional to Ω) in equation (21) as the sum of a zero-rotation part (zero subscript) plus a rotational correction (barred). To first order in Ω,

$$\bar{\sigma} = \frac{-\sigma_0^3 \bar{J} + \sigma_0^2 R_1 + \sigma_0 \bar{\ddot{R}} - R_2 - i\bar{N}}{3\sigma_0^2 J_0 - \ddot{R}_0}. \tag{25}$$

An interesting aspect of this equation is that if any multiple of the zero-rotation integrals is added to the barred integrals (that is, if $\bar{J} \to \bar{J} + nJ_0$, $\bar{\ddot{R}} \to \bar{\ddot{R}} + n\ddot{R}_0$, and $\bar{N} \to \bar{N} + nN_0$ for any number n), the value of $\bar{\sigma}$ remains unchanged. This is because the zero-rotation integrals added to the numerator will exactly cancel by virtue of equation (22).

V. NORMALIZATION OF THE SECOND LINEARIZED EQUATIONS

As mentioned above, the second linearized equations are not homogeneous, and so require a nonarbitrary normalization. The coefficients of the $\bar{y}_i$ are the same as those of the y_{i0} in the zero-rotation equations of Saio and Cox (1980). Thus, if $\bar{y}_i$ is a solution to the second linearized equations, so is $\bar{y}_i + ny_{i0}$ for any complex number n. Changing the value of n is equivalent to changing the normalization of the $\bar{y}_i$.

The procedure followed here consists of solving the second linearized equations with some arbitrary normalization ($\bar{y}_i = 0$ at the surface was used). This yields the eigenvalue C, which is independent of the normalization. These solutions $\bar{y}_i$ are related to the physically correct solutions $\bar{\mathscr{y}}_i$ (whatever they may be) by

$$\bar{y}_i = \bar{\mathscr{y}}_i + ny_{i0}$$

The task is to determine a "correct" value of n. For this purpose an orthogonality condition involving the eigenfunction η (corresponding to the $\bar{\mathscr{y}}_i$) was used:

$$\int \rho \boldsymbol{\xi}_0^* \cdot \boldsymbol{\eta} \, d^3r = 0. \tag{26}$$

Thus,

$$n = \frac{\int \rho \boldsymbol{\xi}_0^* \cdot \bar{\boldsymbol{\xi}} d^3r}{\int \rho \boldsymbol{\xi}_0^* \cdot \boldsymbol{\xi}_0 d^3r},$$

where $\bar{\boldsymbol{\xi}}$ is the eigenfunction corresponding to any arbitrary normalization. The orthogonality condition (26) is the same as that given in Unno et al. (1979, p. 155). Still, it has not been rigorously shown to be the physically relevant one. Equation (26) is equivalent to the statement that the zero-rotation eigenfunction $\boldsymbol{\xi}_0$ contains no

rotational information. This is consistent with the invariance of the integral expression (25) for $\bar{\sigma}$ to the addition of multiples of $\boldsymbol{\xi}_0$ to $\bar{\boldsymbol{\xi}}$, as mentioned at the end of § IV. Physically, the orthogonality condition means that, at least in the adiabatic approximation, the rotational correction to the total energy

$$\bar{E} = \tfrac{1}{2}\sigma_{0r}^2 \bar{J} + \sigma_{0r} \bar{\sigma}_r J_0 - \tfrac{2}{3}\sigma_{0r} R_1$$

(cf. Aizenman and Cox 1975, eq. [61]) is determined solely by the zero-rotation properties of the star. For adiabatic oscillations, $\bar{J}$ is zero by the orthogonality condition, and $\bar{\sigma}$ is determined by the zero-rotation eigenfunctions (see, for example, § 82 of Ledoux and Walraven). Again, it should be stressed that the complex eigenvalue C, which determines the rotational correction to the stability coefficient, is independent of the normalization of the second linearized equations. The $\bar{y}_i$, as determined above, in principle give information on what effect rotation has on the pulsational structure of the star.

VI. NUMERICAL CALCULATIONS

The set of second linearized equations were solved for four stellar models representing an evolutionary sequence followed by a star of 12 $M_\odot$. The models, computed by H. Saio and used with his kind permission, are described in Saio and Cox (1980). Figure 1 shows
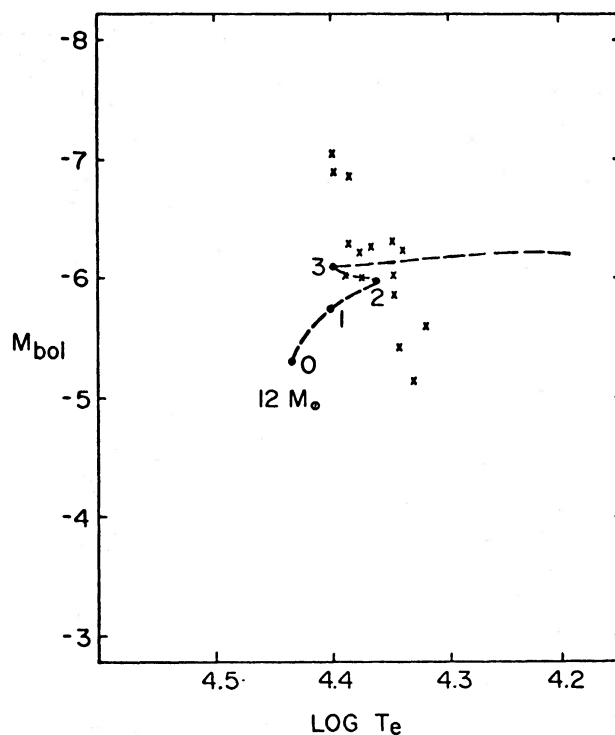
FIG. 1.—Locations on the H-R diagram of the stellar models examined in this paper. The evolutionary track of the 12 $M_\odot$ model is indicated by the dashed line, and the positions of known Beta Cepheid variables are marked with a cross. (Adapted from Saio et al. 1980.)
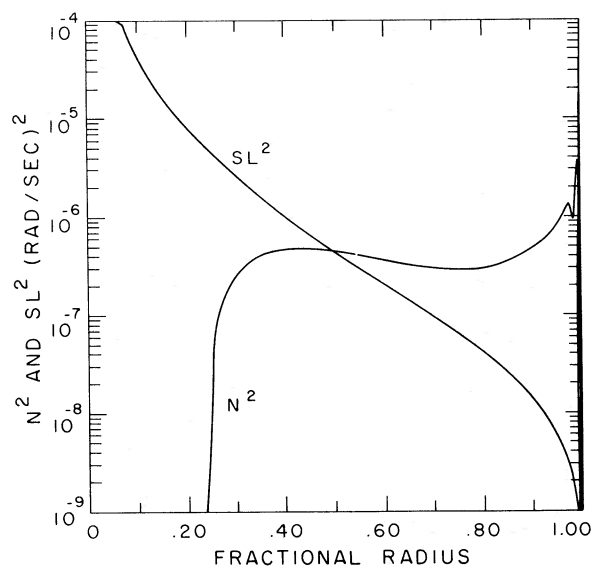
FIG. 2

FIG. 4

FIG. 2.—Propagation diagram for 12 $M_\odot$ Stage 0 (ZAMS) model. The squares of the Brunt-Väisälä frequency N and the critical acoustic frequency Sl are plotted as functions of the fractional radius r/R.

FIG. 4.—Propagation diagram for 12 $M_\odot$ Stage 2 model (same quantities as Fig. 2).
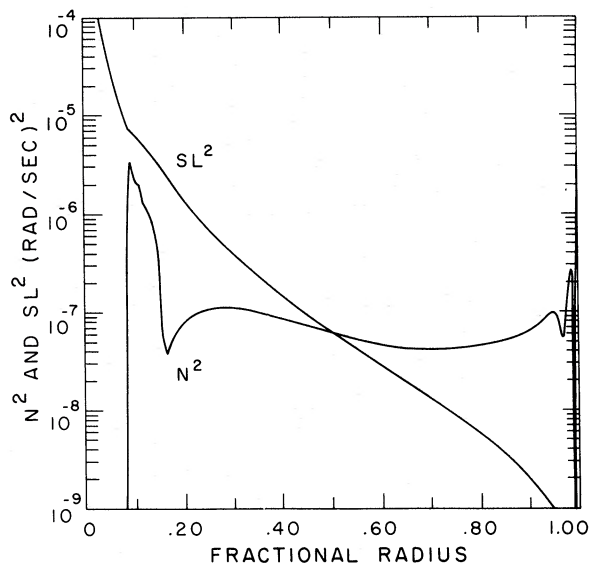
TABLE 1

UNPERTURBED MODELS OF 12 $M_\odot$ STAR ($X = 0.7$, $Z = 0.03$)[a]

Stage	Age (10^7 yr)	$\log(L/L_\odot)$	$\log T_e$ (K)	$\log(R/R_\odot)$	X_{center}
0	0.	4.006	4.435	0.655	0.700
1	1.231	4.191	4.402	0.815	0.303
2	1.613	4.274	4.363	0.934	0.055
3	1.707	4.325	4.400	0.885	0.000

[a] Taken from Saio and Cox 1980.

the path on the H-R diagram followed by these models. This path winds back and forth across the β Cephei instability strip. The locations of the four models are indicated on Figure 1; the crosses mark the locations of known β Cephei variables. Stage 0 is a zero-age main-sequence star having an initial composition of $X = 0.7$ and $Z = 0.03$; Stage 1 is in the late core-hydrogen-burning phase; Stage 2 is at the location of the core hydrogen exhaustion, at the start of the secondary contraction phase; Stage 3 is at the end of the secondary contraction phase, at the onset of hydrogen shell burning.
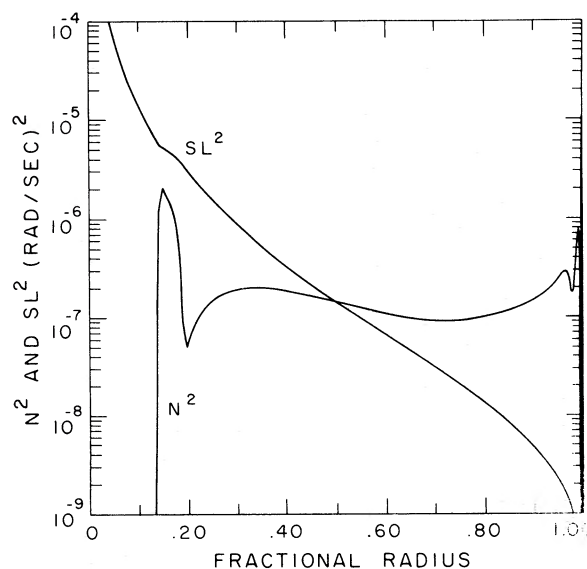
FIG. 3.—Propagation diagram for 12 $M_\odot$ Stage 1 model (same quantities as Fig. 2).
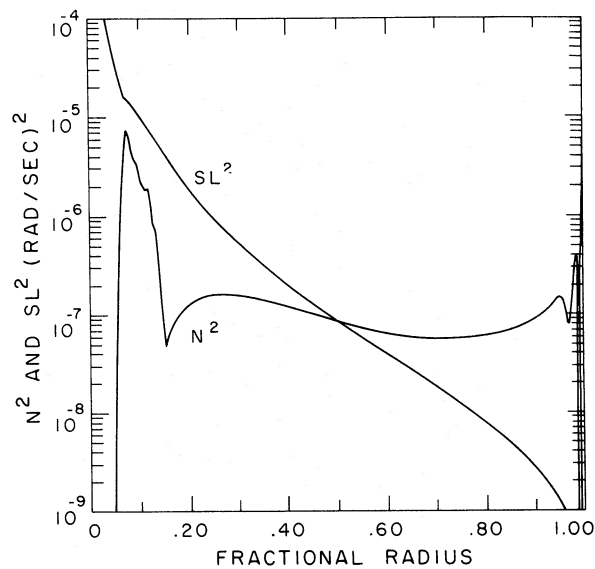
FIG. 5.—Propagation diagram for 12 $M_\odot$ Stage 3 model (same quantities as Fig. 2).
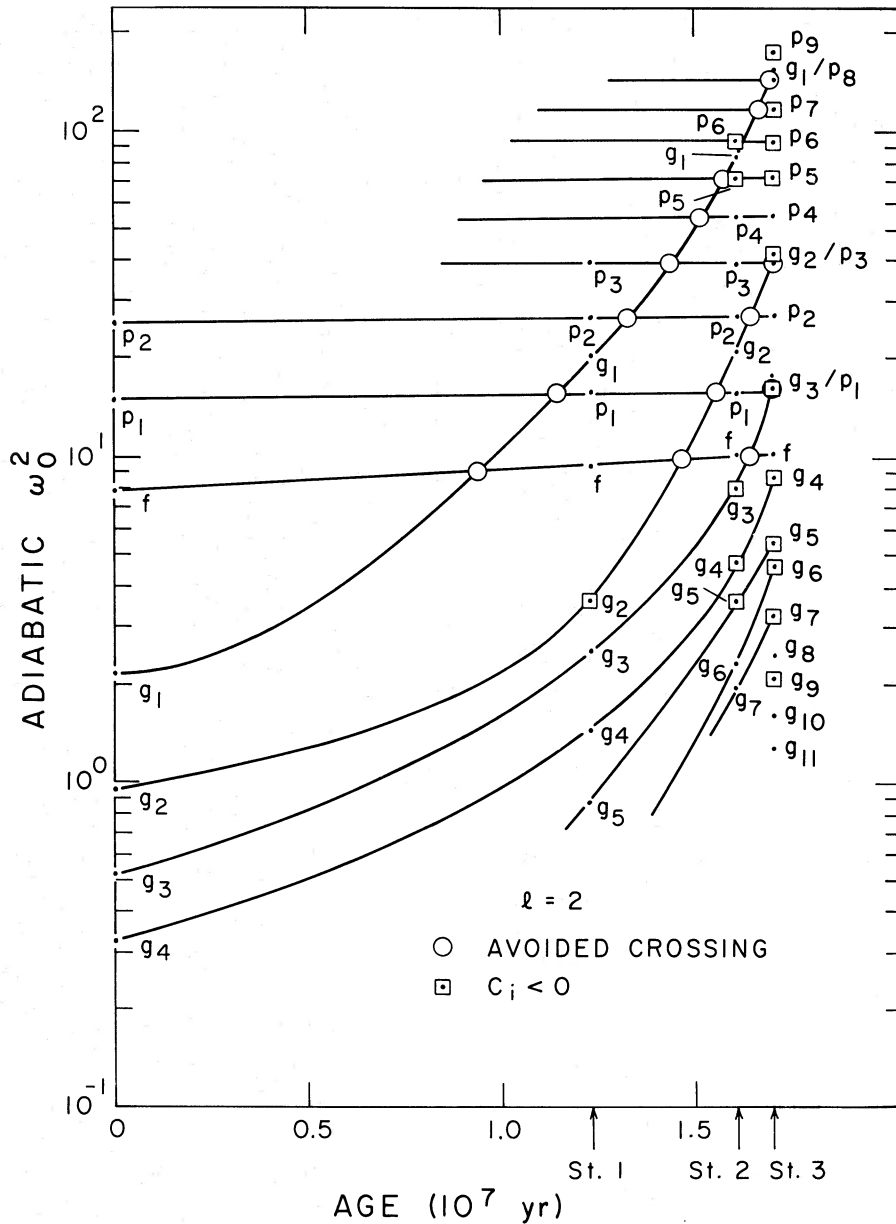
FIG. 6.—Evolution diagram for 12 $M_\odot$ models, $l = 2$. The square of the dimensionless adiabatic pulsation frequency is plotted as a function of evolutionary age.

Table 1 gives a brief summary of the properties of these four models.

A propagation diagram is plotted for each model (Figs. 2–5). These diagrams display the values of N^2, the square of the Brunt-Väisälä frequency,

$$N^2 = -Ag ,$$

and Sl^2 the square of the critical acoustic frequency,

$$Sl^2 = \frac{l(l+1)\Gamma_1 P}{r^2\rho} ,$$

throughout the star. For a nonrotating star, a local analysis shows that a wave of frequency σ can propagate only in those regions where

$$\sigma^2 > N^2 , \quad \sigma^2 > Sl^2 \quad (p \text{ modes}) ,$$

or

$$\sigma^2 < N^2 , \quad \sigma^2 < Sl^2 \quad (g \text{ modes}) .$$

Otherwise, the wave is evanescent. The effect of rotation on this scheme will be discussed below.

The numerical solutions to the set of second linearized differential equations were calculated using a Newton-Raphson relaxation program. First the zero-rotation

equations were solved, then these solutions were used to find the rotational corrections. The integral expressions described in § IV were evaluated as a check on the eigenfunctions. Good agreement between the eigenvalues and integrated values was usually obtained.

Solutions were found for all modes having $l = 2$ or 3 and periods between 2 and 15 hours. The results for 125 modes are summarized in an extensive appendix in Carroll (1981). Figures 6 and 7 show ω_0^2, the square the dimensionless adiabatic pulsation frequency (without rotation), plotted as a function of the age of the stellar model. These "evolution diagrams" display the avoided crossings (circled) discussed by Osaki (1975) and Aizenman, Smeyers, and Weigert (1977), among others. Although the shapes of the lower parts of the curves is only a qualitative estimate, the confluence of the $l = 3$ g_3 and g_4 modes between Stages 2 and 3 may be an avoided crossing. These diagrams also distinguish those modes for which C_i, the imaginary part of the eigenvalue C, is negative. The number of modes with $C_i > 0$ increases dramatically as the star evolves.

The "pulsation constant" $Q = (\text{Period})(\bar{\rho}/\bar{\rho}_\odot)^{1/2}$
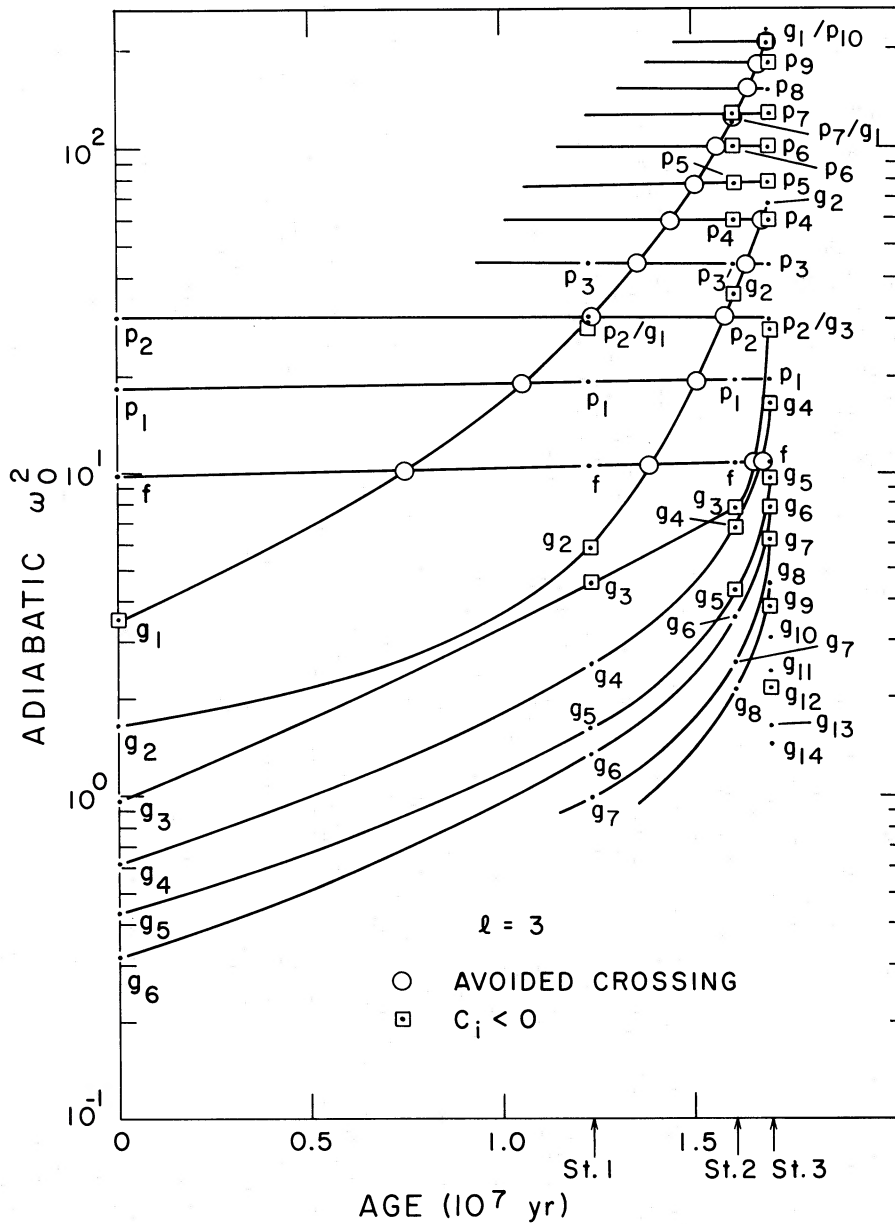
FIG. 7.—Evolution diagram for 12 $M_\odot$ models, $l = 3$ (same quantities as Fig. 6)
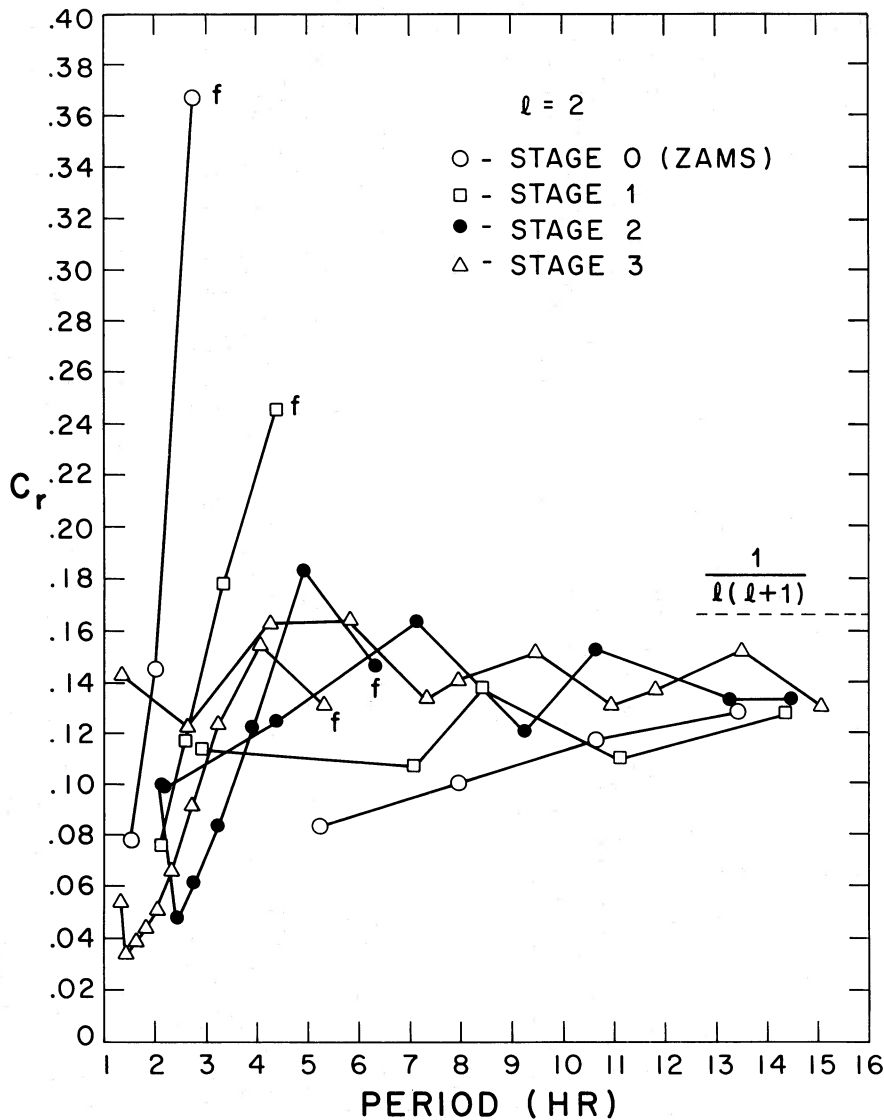
FIG. 8.—The real part of the eigenvalue C plotted as a function of the pulsation period for each 12 $M_\odot$, $l = 2$ mode. The f mode for each model is connected to the p modes by a solid line. Another line connects the g modes for each model.

(where $\bar\rho$ and $\bar\rho_\odot$ are the mean densities of the star and Sun, respectively) is proportional to $1/\omega_0$ (see eq. [14]). From Figures 6 and 7, it is clear that Q is a constant only for the f and p modes. For the g modes, Q decreases with time (by as much as a factor of 5) in response to the increasing gradient of the mean molecular weight in the core of the star.

Figures 8 and 9 show C_r, the real part of the eigenvalue C, plotted as a function of the pulsation period for each of the 12 $M_\odot$ models. As the period increases, the values of C_r begin to converge to their asymptotic value of $1/[l(l + 1)]$ (see § 19.1c of Cox 1980). Although C_r is positive for all modes shown in these two figures, two negative values of C_r were found for the $l = 4$ g_1 and g_2 modes. The sign and magnitude of C_r may be understood by examining the effect of the Coriolis force on the

propagation diagrams, Figures 2–5. Following § 14 of Unno et al. (1979), we define

$$\zeta = r^3 y_1 \exp\left[-\int_0^r \frac{1}{r'}\left(\frac{V}{\Gamma_1} + \frac{2m\Sigma}{\omega}\right)dr'\right] ,$$

$$\eta = gr y_2 \exp\left[\int_0^r \frac{1}{r'}\left(r'A + \frac{2m\Sigma}{\omega}\right)dr'\right] .$$

For adiabatic motion in the Cowling approximation ($\psi' \equiv 0$), equations (15) and (16) may be written as

$$\frac{d\zeta}{dr} = \eta\left[\frac{Sl_{\mathrm{eff}}^2}{\sigma^2} - 1\right]\frac{r^2\rho}{\Gamma_1 P}$$

$$\times \exp\left[-\int_0^r \frac{1}{r'}\left(\frac{V}{\Gamma_1} + r'A + \frac{4m\Sigma}{\omega}\right)dr'\right] , \quad (27)$$
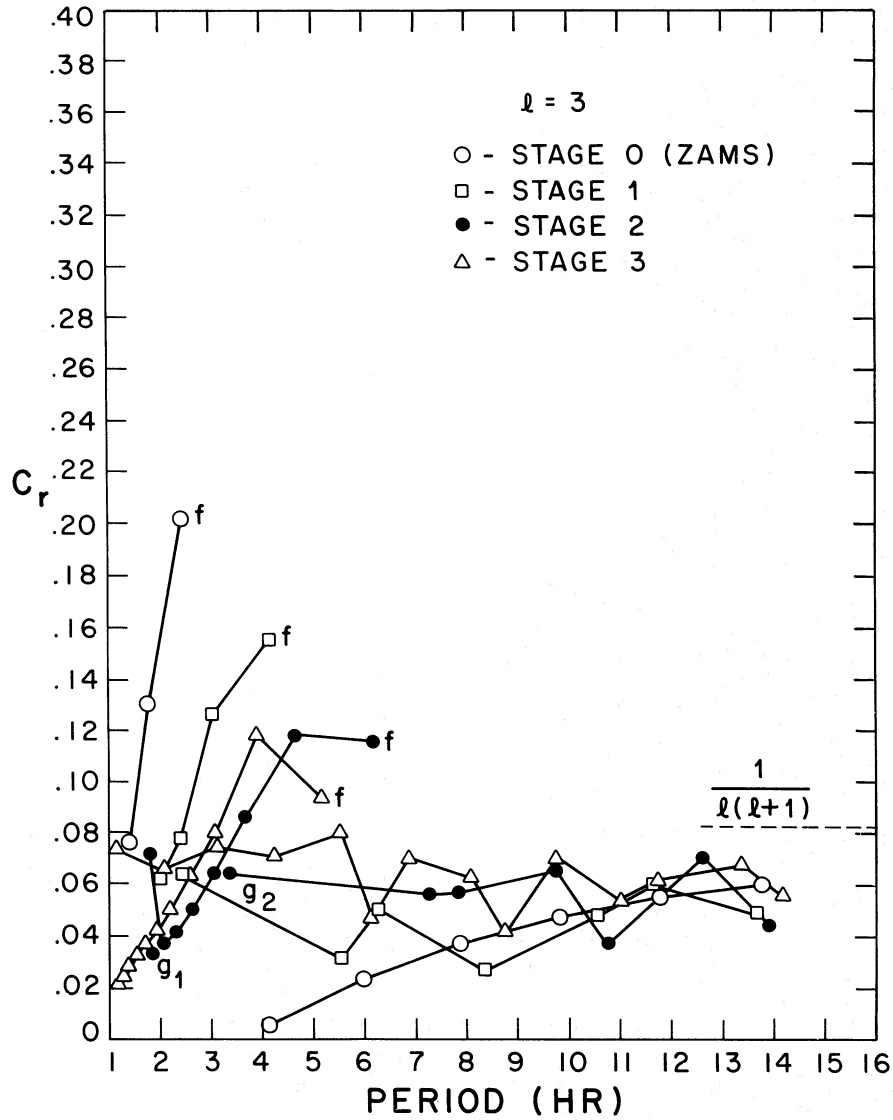
FIG. 9.—The real part of the eigenvalue C plotted as a function of the pulsation period for each 12 $M_\odot$, $l = 3$ mode (same quantities as Fig. 6).

$$\frac{d\eta}{dr} = \zeta \left[\frac{\sigma^2}{N_{\text{eff}}^2} - 1 \right] \left(\frac{-Ag}{r^2} \right)$$

$$\times \exp\left[\int_0^r \frac{1}{r'} \left(\frac{V}{\Gamma_1} + r'A + \frac{4m\Sigma}{\omega} \right) dr' \right], \quad (28)$$

where Sl_{eff}^2 is the square of the effective critical acoustic frequency

$$Sl_{\text{eff}}^2 = \frac{l(l+1)\Gamma_1 P}{r^2 \rho} \left[1 - \frac{2m\Sigma}{\omega} \left(1 - \frac{1}{l(l+1)} \right) \right],$$

and N_{eff}^2 is the square of the effective Brunt-Väisälä frequency

$$N_{\text{eff}}^2 = -Ag\left(1 - \frac{2m\Sigma}{\omega} \right).$$

For a local analysis, everything except ζ and η is set equal to its local value, and ζ and η are assumed to vary as $\exp[ik_r r]$, where k_r is the local radial wavenumber. Then equations (27) and (28) lead to

$$k_r^2 = \frac{1}{r^2} rA \frac{V}{\Gamma_1} \left[\frac{Sl_{\text{eff}}^2}{\sigma^2} - 1 \right] \left[\frac{\sigma^2}{N_{\text{eff}}^2} - 1 \right].$$

A wave can propagate only if $k_r^2 > 0$. Recalling that A is negative (except in a convection zone), it is seen that $k_r^2 > 0$, if

$$\sigma^2 > N_{\text{eff}}^2, \quad \sigma^2 > Sl_{\text{eff}}^2 \quad (p \text{ modes}),$$

or if

$$\sigma^2 < N_{\text{eff}}^2, \quad \sigma^2 < Sl_{\text{eff}}^2 \quad (g \text{ modes}).$$

Otherwise, the wave is evanescent.

If $m > 0$, then both Sl_{eff}^2 and N_{eff}^2 are reduced below their zero-rotation values, while the opposite is true if $m < 0$. Thus both curves in Figures 2–5 are either lowered (if $m > 0$) or raised (if $m < 0$) by the effect of the Coriolis force. The result is that the pulsation frequencies are decreased below (increased above) their zero-rotation values for $m > 0$ ($m < 0$). From equations (19), this means that $C_r < 1$ (as is certainly true for a nonrotating star). This is indeed true for all modes examined. Repeating this argument in a corotating frame leads to the conclusion that, almost always, $C_r > 0$. Again, this is confirmed by the numerical calculations.

Figures 10 and 11 show the ratio $|\bar{\kappa}/\kappa_0|$ in units of $2m\Omega/\sigma_0$ for $l = 2, 3$ plotted as a function of the pulsation period for each of the 12 $M_\odot$ models. Arrows indicate those models for which $C_i < 0$. No clear trend is evident: although it is tempting to believe that the sign of C_i is randomly determined for the Stage 2 and 3 models, this

cannot be true for the younger Stage 0 and 1 models, which predominantly have $C_i > 0$. These results are in agreement with the quasi-adiabatic calculations of HCC. Unfortunately, the attempts at understanding the physical basis for the sign of C_i have so far been unsuccessful. The effect of the Coriolis force, which is the only one that slow rotation introduces, is not to do any direct work on the star since it is perpendicular to the velocity vector. As conjectured in HCC, the effect must be indirect such as a basic modification of the eigenfunctions.

The sign of C_i may possibly be relevant to the evolutionary status of the β Cephei variables. As mentioned above, as a star of the appropriate mass (roughly between 10 and 20 $M_\odot$) evolves away from the main sequence, it traces out an S shaped track (shown in Fig. 1) as it travels back and forth through an instability strip. All but 3% of a star's lifetime in the
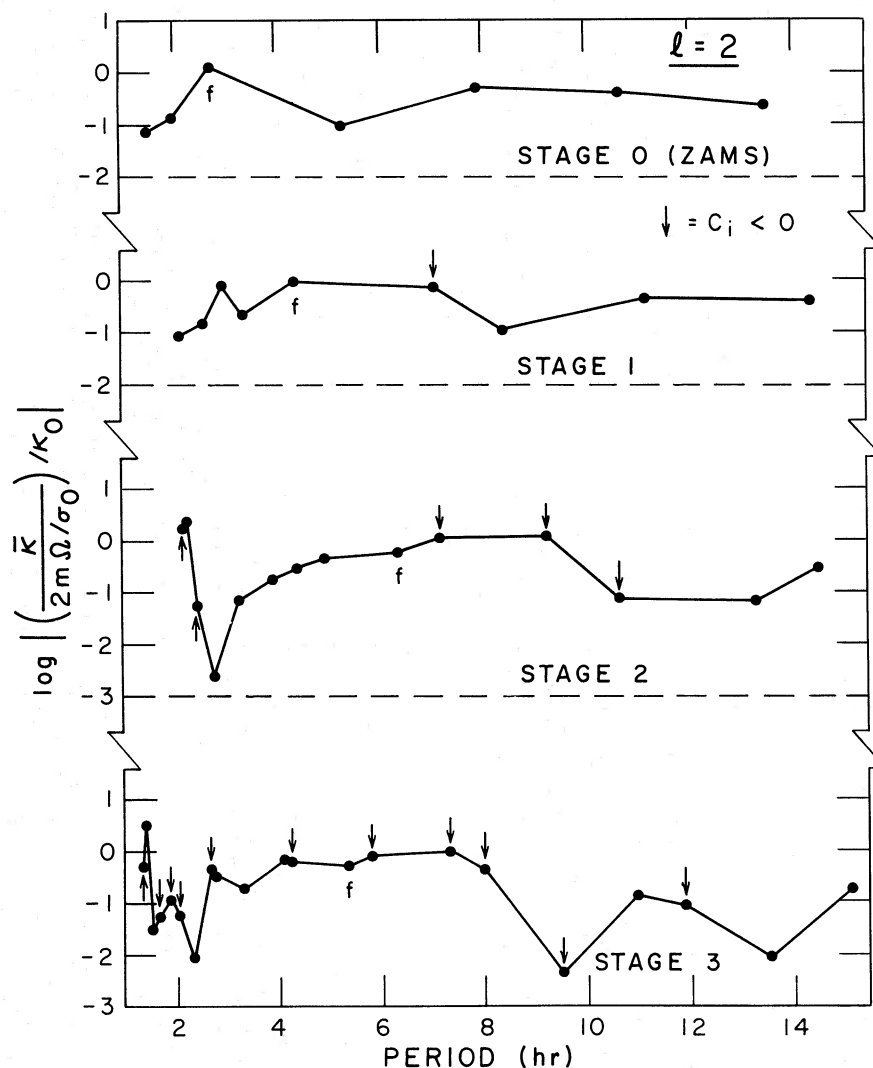
FIG. 10.—The ratio $|\bar{\kappa}/\kappa_0|$ in units of $2m\Omega/\sigma_0$ as a function of the pulsation period for each 12 $M_\odot$, $l = 2$ mode. The f mode for each model is indicated.
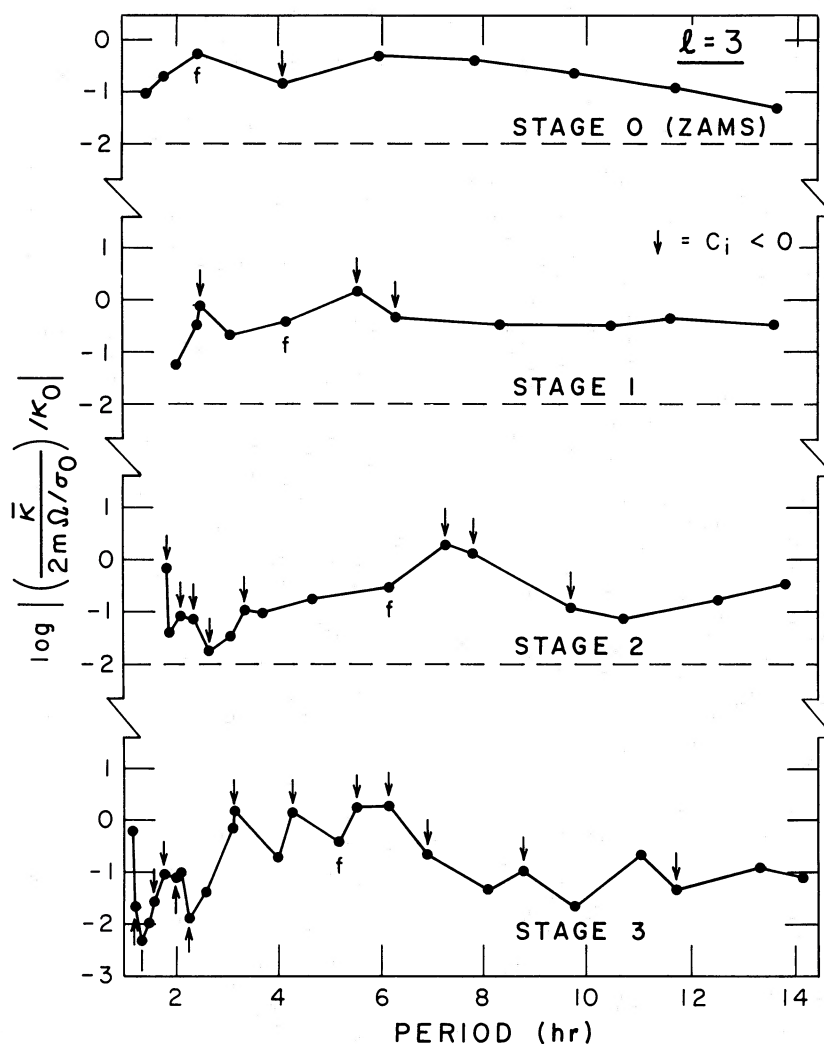
FIG. 11.—The ratio $|\bar{\kappa}/\kappa_0|$ in units of $2m\Omega/\sigma_0$ as a function of the pulsation period for each 12 $M_\odot$, $l = 3$ mode. The f mode for each model is indicated.

strip occurs during the core-hydrogen-burning phase of its evolution. Because most of the stars in the strip appear to be variable (Sterken and Jerzykiewicz 1980), it is likely that the β Cephei stars are in the longer lasting core-hydrogen-burning phase. (However, Lesh and Aizenman 1978 point out the difficulty in making such a statistical argument.) The periodic changes in the line profiles seen in β Cephei stars allow prograde ($m < 0$) and retrograde ($m > 0$) pulsation modes to be clearly distinguished (Smith 1980a). In almost all cases where a probable mode identification has been made, m has been negative, with the $m = -l$ mode usually present. (See, for example, Smith 1980b and Saio 1981).

If the observational preference for negative m values has been correctly identified, and if rotationally split modes having $\bar{\kappa} < 0$ are truly preferentially excited, then equation (20) shows that $C_i > 0$ for almost all of the modes seen in the β Cephei stars. Furthermore, if the

stellar models used (which are not pulsationally unstable; none exist which are) allow an accurate determination of the sign of C_i for the β Cephei stars, then we can infer that these stars are probably nearer to Stage 1 in their evolution than to Stages 2 and 3. Otherwise, both positive and negative values of m should be observed. However, because this comes after several caveats, the most that can be said is that this conclusion is consistent with the statement that the β Cephei variables are in the core-hydrogen-burning phase of their evolution.

APPENDIX

The full set of second linearized equations and boundary conditions referred to in § III are given below:

$$r\frac{d\bar{y}_1}{dr} = \left[\frac{V}{\Gamma_1} - 3\right]\bar{y}_1 + \left[\frac{l(l+1)}{C_1\omega_0^2} - \frac{V}{\Gamma_1}\right]\bar{y}_2 + \frac{V}{\Gamma_1}\bar{y}_3 + \frac{\chi_T}{\chi_\rho}\frac{4}{4+i\omega_0 C_4}\bar{Y}_5$$

$$+ \frac{2m\Sigma}{\omega_0}\left\{y_{10} + \frac{1}{C_1\omega_0^2}[1 - Cl(l+1)]y_{20} - \frac{\chi_T}{\chi_\rho}\frac{2iC\omega_0 C_4}{(4+i\omega_0 C_4)^2}Y_{50}\right\},$$

$$r\frac{d\bar{y}_2}{dr} = [C_1\omega_0^2 + rA]\bar{y}_1 + [1 - U - rA]\bar{y}_2 + rA\bar{y}_3 + \frac{\chi_T}{\chi_\rho}\frac{4}{4+i\omega_0 C_4}\bar{Y}_5$$

$$+ \frac{2m\Sigma}{\omega_0}\left\{C_1\omega_0^2 Cy_{10} - y_{20}, \quad -\frac{\chi_T}{\chi_\rho}\frac{2iC\omega_0 C_4}{(4+i\omega_0 C_4)^2}Y_{50}\right\},$$

$$r\frac{d\bar{y}_3}{dr} = (1 - U)\bar{y}_3 + \bar{y}_4,$$

$$r\frac{d\bar{y}_4}{dr} = -rAU\bar{y}_1 + \frac{UV}{\Gamma_1}\bar{y}_2 + \left[l(l+1) - \frac{UV}{\Gamma_1}\right]\bar{y}_3 - U\bar{y}_4 - U\frac{\chi_T}{\chi_\rho}\frac{4}{4+i\omega_0 C_4}\bar{Y}_5 + \frac{2m\Sigma}{\omega_0}U\frac{\chi_T}{\chi_\rho}\frac{2iC\omega_0 C_4}{(4+i\omega_0 C_4)^2}Y_{50},$$

$$\frac{1}{\nabla V}r\frac{d\bar{Y}_5}{dr} = [B_1 + \alpha(U - C_1\omega_0^2) + 4(1-\alpha)]\bar{y}_1 - \left[B_1 + \frac{l(l+1)}{C_1\omega_0^2}(1-\alpha)\right]\bar{y}_2$$

$$+ B_1\bar{y}_3 + \alpha\bar{y}_4 + 4\left[\frac{(\chi_T/\chi_\rho)\kappa_\rho - \kappa_T}{4+i\omega_0 C_4} + 1\right]\bar{Y}_5 - \bar{y}_6$$

$$+ \frac{2m\Sigma}{\omega_0}\left\{[\alpha(1 - C_1\omega_0^2 C) - 1]y_{10} + \left[\frac{\alpha-1}{C_1\omega_0^2}(1 - Cl(l+1)) + \alpha\right]y_{20} - 2iC\omega_0 C_4\frac{(\chi_T/\chi_\rho)\kappa_\rho - \kappa_T}{(4+i\omega_0 C_4)^2}Y_{50}\right\}$$

$$r\frac{d\bar{y}_6}{dr} = -[B_2 + (1-\alpha)l(l+1)]\bar{y}_1 + \left[B_2 - \alpha l(l+1) + \eta\frac{l(l+1)}{C_1\omega_0^2}\right]\bar{y}_2 - [B_2 - \alpha l(l+1)]\bar{y}_3$$

$$+ \left[4\left(\frac{B_3 - i\omega_0 B_4}{4+i\omega_0 C_4}\right) - \frac{l(l+1)}{\nabla V}\right]\bar{Y}_5 - \eta\bar{y}_6 + \frac{2m\Sigma}{\omega_0}\left\{\eta y_{10} + \frac{\eta}{C_1\omega_0^2}(1 - Cl(l+1))y_{20}\right.$$

$$\left. - 2iC\omega_0 C_4\frac{4B_4 + B_3 C_4}{(4+i\omega_0 C_4)^2}Y_{50}\right\}.$$

In these equations,

$$Y_5 \equiv \left[1 + \frac{i(\omega + m\Sigma)C_4}{4}\right]y_5.$$

All other quantities are as defined in Saio and Cox (1980).

The boundary conditions at the stellar center are

$$C_1\omega_0^2\bar{y}_1 - l\bar{y}_2 + \frac{2m\Sigma}{\omega_0}\left(C - \frac{1}{l}\right)y_{10} = 0,$$

$$l\bar{y}_3 - \bar{y}_4 = 0,$$

and

$$\bar{Y}_5 \propto r^l.$$

Those at the surface are

$$U\bar{y}_1 + (l+1)\bar{y}_3 + \bar{y}_4 = 0,$$

$$[V - C_1\omega_0^2 - 4]\bar{y}_1 + \left[\frac{l(l+1)}{C_1\omega_0^2} - V\right]\bar{y}_2 + [V - (l+1)]\bar{y}_3$$

$$+ \frac{2m\Sigma}{\omega_0}\left\{[1 - C_1\omega_0^2 C]y_{10} + \left[\frac{1}{C_1\omega_0^2}(1 - Cl(l+1)) + 1\right]y_{20}\right\} = 0,$$

$$(2 - 4\nabla_{ad}V)\bar{y}_1 + 4\nabla_{ad}V(\bar{y}_2 - \bar{y}_3) + 4\bar{Y}_5 - \bar{y}_6 = 0.$$

The expressions for the components of the Lagrangian displacement ξ, equations (8)–(10), indicate that the velocity of a mass element in a rotating pulsating star is not simply the sum of its zero-rotation pulsation velocity plus the velocity of rotation $\Omega r \sin \theta \hat{\phi}$. Nevertheless, it is this form of the surface velocity field that it most often used in attempts to theoretically fit the observed line profiles of such stars (see, for example, Osaki 1971; Smith and McCall 1978).

A more exact expression for the components of the velocity of a mass element, seen from an intertial frame and accurate to first order in Ω, is

$$\frac{1}{N_{lm}} v_r = - |a_0|(\kappa_0 + m\Omega C_i)P_l^m \cos(\sigma_r t + m\phi + \phi_{a0}) - |a_0|(\sigma_{0r} + m\Omega C_r)P_l^m \sin(\sigma_r t + m\phi + \phi_{a0})$$

$$- |\hat{a}|\kappa_0 P_l^m \cos(\sigma_r t + m\phi + \hat{\phi}_a) - |\hat{a}|\sigma_{0r} P_l^m \sin(\sigma_r t + m\phi + \hat{\phi}_a) + |b_0|m\Omega P_l^m \sin(\sigma_r t + m\phi + \phi_{b0}),$$

$$\frac{1}{N_{lm}} v_\theta = - |b_0|(\kappa_0 - m\Omega C_i)\left(\frac{d}{d\theta} P_l^m\right)\cos(\sigma_r t + m\phi + \phi_{b0})$$

$$- |b_0|\left[(\sigma_{0r} - m\Omega C_r)\left(\frac{d}{d\theta} P_l^m\right) + m\Omega \frac{\cos\theta}{\sin\theta} P_l^m\right]\sin(\sigma_r t + m\phi + \phi_{b0})$$

$$- |\bar{b}|\kappa_0\left(\frac{d}{d\theta} P_l^m\right)\cos(\sigma_r t + m\phi + \bar{\phi}_b) - |\bar{b}|\sigma_{0r}\left(\frac{d}{d\theta} P_l^m\right)\sin(\sigma_r t + m\phi + \bar{\phi}_b),$$

$$\frac{1}{N_{lm}} v_\phi = \frac{1}{N_{lm}}\Omega r \sin\theta - |a_0|\Omega \sin\theta P_l^m \cos(\sigma_r t + m\phi + \phi_{a0}) - |b_0|\left[(\sigma_{0r} - m\Omega C_r)\frac{m}{\sin\theta} P_l^m + \Omega \cos\theta\left(\frac{d}{d\theta} P_l^m\right)\right]$$

$$\times \cos(\sigma_r t + m\phi + \phi_{b0}) + |b_0|(\kappa_0 - m\Omega C_i)\frac{m}{\sin\theta} P_l^m \sin(\sigma_r t + m\phi + \phi_{b0})$$

$$- |\bar{b}|\sigma_{0r}\frac{m}{\sin\theta} P_l^m \cos(\sigma_r t + m\phi + \bar{\phi}_b) + |\bar{b}|\kappa_0 \frac{m}{\sin\theta} P_l^m \sin(\sigma_r t + m\phi + \bar{\phi}_b).$$

In deriving the above expressions, the spherical harmonics were written as

$$Y_l^m = N_{lm}P_l^m(\cos\theta)e^{im\phi},$$
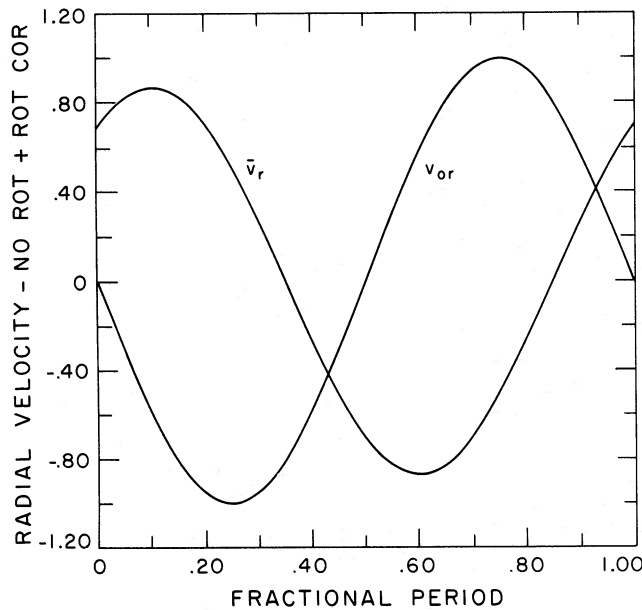
FIG. 12.—The zero-rotation radial velocity v_{0r} and the rotational correction $\bar{v}_r$ plotted as functions of the fractional pulsation period for the 12 $M_\odot$ Stage 2, $l = 3$, g_3 mode. v_{0r} is normalized to unity, and $\bar{v}_r$ must be multiplied by the appropriate value of $2m\Omega/|\sigma_0|$.

where

$$N_{lm} = \left(\frac{2l+1}{4\pi} \frac{(l-m)!}{(l+m)!} \right)^{1/2}$$

and P_l^m is the associated Legendre function. The quantities a_0 and b_0 are those defined by equations (11)–(13),

$$a_0 = r y_{10} , \qquad b_0 = \frac{g}{\sigma_0^2} y_{20} ,$$

and

$$\hat{a} \equiv r \bar{y}_1 , \qquad \bar{b} \equiv \frac{g}{\sigma_0^2} \bar{y}_2 .$$

These complex quantities were written in exponential form, $f = |f| \exp [i\phi_f]$. Surface values of the magnitudes and arguments of a_0, b_0, $\hat{a}$, and $\bar{b}$ for each mode are compiled in the Appendix of Carroll (1981). The coefficient σ_r of the time t is the sum of the zero-rotation and rotational correction contributions: $\sigma_r = \sigma_{0r} + \bar{\sigma}_r$. Figure 12 shows a typical plot of the zero-rotation radical velocity v_{0r}, plus the rotational correction $\bar{v}_r$. In the diagram, v_{0r} is normalized to unity, and $\bar{v}_r$ must be multiplied by $2m\Omega/|\sigma_0|$ before it is added to v_{0r}.

REFERENCES

Aizenman, M. L., and Cox, J. P. 1975, *Ap. J.*, **202**, 137.
Aizenman, M. L., and Smeyers, P. 1977, *Ap. Space Sci.*, **48**, 123.
Aizenman, M. A., Smeyers, P., and Weigert, A. 1977, *Astr. Ap.*, **58**, 41.
Carroll, B. W. 1981, Ph.D. thesis, University of Colorado.
Cox, J. P. 1980, *Theory of Stellar Pulsation* (Princeton: Princeton University Press).
Hansen, C. J., Cox, J. P., and Carroll, B. W. 1978, *Ap. J.*, **226**, 210 (HCC).
Hansen, C. J., Cox, J. P., and Van Horn, H. M. 1977, *Ap. J.*, **217**, 151.
Ledoux, P., and Walraven, T. 1958, in *Handbuch der Physik*, ed. S. Flügge (Berlin: Springer-Verlag), Vol. **51**, p. 353.
Lesh, J. R., and Aizenman, M. L. 1978, *Ann. Rev. Astr. Ap.*, **16**, 215.
Lynden-Bell, D., and Ostriker, J. P. 1967, *M.N.R.A.S.*, **136**, 293.
Osaki, Y. 1971, *Pub. Astr. Soc. Japan*, **23**, 485.
———. 1975, *Pub. Astr. Soc. Japan*, **27**, 237.
Saio, H. 1981, *Ap. J.*, **244**, 299.
Saio, H., and Cox, J. P. 1980, *Ap. J.*, **236**, 549.

Saio, H., Cox, J. P., Hansen, C. J., and Carroll, B. W. 1980, in *Proceedings of the Workshop on Nonradial and Nonlinear Stellar Instabilities*, ed. H. Hill and W. Dziembowski (New York: Springer-Verlag), p. 13.
Smith, M. A. 1980a, in *Current Problems in Stellar Pulsation Instabilities*, ed. D. Fischel, J. R. Lesh, and W. M. Sparks (NASA Tech. Memo. 80625), p. 391.
———. 1980b, *Ap. J.*, **240**, 149.
Smith, M. A., and McCall, M. L. 1978, *Ap. J.*, **223**, 221.
Sterken, C., and Jerzykiewicz, M. 1980, in *Proceedings of the Workshop on Nonradial and Nonlinear Stellar Instabilities*, ed. H. Hill and W. Dziembowski (New York: Springer-Verlag), p. 105.
Unno, W. 1965, *Pub. Astr. Soc. Japan*, **17**, 205.
Unno, W., and Spiegel, E. A. 1966, *Pub. Astr. Soc. Japan*, **18**, 85.
Unno, W., Osaki, Y., Ando, H., and Shibahashi, H. 1979, *Nonradial Oscillations of Stars* (Tokyo: Tokyo University Press).

BRADLEY W. CARROLL: Department of Physics and Astronomy, University of Rochester, Rochester, NY 14627

CARL J. HANSEN: Department of Astro-Geophysics, University of Colorado, Boulder, CO 80309